Supporting Information

Regulation of Redox Balance Enhances Phototherapy Efficacy and Suppresses Tumor Metastasis Using a Biocompatible Nanoplatform

Qunying Jiang,[a] Min Pan,[a] Jialing Hu,[a] Junlin Sun,[a] Lei Fan,[a] Zhiqiao Zou,[a] Jianshuang Wei,[b] Xiaoquan Yang,[b] and Xiaoqing Liu*[a]

[a]Key Laboratory of Analytical Chemistry for Biology and Medicine (Ministry of Education), College of Chemistry and Molecular Sciences, Wuhan University, Wuhan, Hubei 430072, P. R. China

[b]Britton Chance Center for Biomedical Photonics, Wuhan National Laboratory for Optoelectronics, Huazhong University of Science and Technology, Wuhan, Hubei 430074, P. R. China

*Corresponding Author: xiaoqingliu@whu.edu.cn

Table of Contents

Materials and instrumentation

Chemicals. Dopamine hydrochloride was purchased from Aladdin Biochemical Technology Co., Ltd (Shanghai, China). Methylene blue (MB) and 1,3-diphenylisobenzofuran (DPBF) were purchased from Sigma-Aldrich (MO, USA). 3-(4,5-Dimethyl-2-thiazolyl)-2,5-diphenyl-2-H-tetrazolium bromide (MTT), 4',6-diamidino-2-phenylindole (DAPI), and 2',7'-dichlorofluorescein diacetate (DCFH-DA) were purchased from Beyotime (China). Dulbecco's modified Eagle's medium (DMEM) with high glucose was purchased from HyClone. Fetal bovine serum was purchased from Biological Industries. Penicillin-streptomycin (100×) was obtained from Life Technologies Corporation (LA, USA). Deionized (DI) water was generated using a Millipore Milli-Q system (Billerica, MA).

Instruments. UV-Vis absorption spectra were recorded by a UV-2600 Shimadzu spectroscope. The sizes and zeta potentials of the nanoparticles were obtained on a Malvern zetasizer (ZEN3690, Malvern, UK). TEM images were captured using an energy-filtering transmission electron microscope (JEM-1400plus) with an accelerating voltage of 120 kV. SEM images were obtained using a field-emission scanning electron microscope (Zeiss Merlin Compact). FT-IR spectrum were measured by a NICOLET 5700 FTIR Spectrometer. CLSM images were captured on a spinning-disk confocal microscope system (PerkinElmer UltraVIEW VoX, America). Fluorescence images were captured by Cytation™ 5 Cell Imaging Multi-Mode

Reader (Biotek, Winooski, VT). Flow cytometry analysis was conducted by flow cytometer (Beckman Coulter Cyto-FLEX™ (CytoFLEXS)).

Experimental procedures

Synthesis of PDA and PDA-MB. In a typical synthesis of polydopamine spheres with an average diameter of 90 nm, ammonium hydroxide (3 mL, NH_4OH) was added into a solution of ethanol (40 mL) and H_2O (90 mL) under mile stirring at 30 ℃ for 30 min [43]. Dopamine hydrochloride (0.5 g) was dissolved in deionized water (10 mL), and then the solution was added into the above mixture. The color of the mixture solution turned to dark brown gradually. The reaction was allowed to proceed for 24 h at 30 ℃ with mile stirring. The product was obtained by centrifuging at 10000 rpm for 10 min and washing with water for five times. The polydopamine was dispersed in H_2O (10 mL) and stored at 4 ℃ until further use. The PDA-MB was prepared through mixing PDA and MB under stirring condition. Briefly, 0.1 mL of PDA (4 mg mL^{-1}) was added into a 3.8 mL aqueous solution containing MB (50, 100, 200, 300, 400, 600, and 1000 μg) under stirring at 700 rpm for 30 min at room temperature. The obtained solutions were centrifuged at 10000 rpm for 10 min and washed with water until the supernatant turning to colorless. Finally, the product was stored at 4 ℃ for further use.

The loading amount of MB on the PDA was calculated by subtracting the amount of MB in all supernatant after centrifugation from the amount of MB the primary reaction solution. The MB Loading efficiency was calculated based on the following Eq (1)

$$\text{Loading efficiency} = (W_{\text{primary MB}} - W_{\text{MB in supernatant}})/W_{\text{primary MB}} * 100\% \quad (1)$$

$W_{primary\ MB}$ presents the primary weight of MB added in system. $W_{MB\ in\ supernatant}$ presents the supernatant of PDA-MB after incubating for 2h.

MB Release in different physiological conditions. For time-dependent release of MB from PDA-MB upon addition of GSH, the study was conducted as follows: 200 μL of PDA-MB (1 mg mL^{-1}) was added in 800 μL aqueous containing of different concentration GSH (0, 0.02, 1, 2 and 10 mM). At different time intervals, 20 μL of solutions was withdrawn from the solution and diluted with water to 200 μL. The amount of the released MB was analyzed by measuring the fluorescence intensity of MB at 640 nm. The MB release efficiency was calculated based on the following Eq (2):

$$\text{Release efficiency} = (MB_{released})/(MB_{loaded})*100\% \quad (2)$$

$MB_{released}$ and MB_{loaded} present the weight of MB.

For time-dependent release of MB from PDA-MB at different pH (5.0, 6.5 and 7.4), H_2O_2 concentrations (0.1,0.2 and 0.5 mM), and mediums (10% serum and 5% BSA), the method was the same as the above.

For the quantitive analysis of released MB levels from PDA-MB with GSH stimulus to normalize MB's contribution to ROS, we measured the fluorescence intensity of MB in supernatant in different systems (free MB, free MB with GSH, PDA-MB, and PDA-MB with GSH). Among of them, PDA-MB (100 μg mL^{-1}) and free MB (100 μg mL^{-1}) were incubated with 1 mM GSH respectively for 30 min before centrifuging for fluorescence measurement.

GSH Depletion Ability of PDA. 5,5'-dithiobis-(2-nitrobenzoic acid) (DTNB) mixture can react with GSH to produce 2-nitro-5-thiobenzoic acid (TNB) whose absorption weak at 412 nm. First, different concentration of GSH were incubated with 100 μg mL^{-1} of PDA for 1 h. Then, 10 μL of above solution diluted to 150 μL with H_2O and introduced 50 μL of 0.4 mg mL^{-1} DTNB. After reaction for 10 min, we measured the absorption of TNB at 412 nm *via* microplate reader. 50 μL of GSH (200 mM) was added into 950 μL PDA and PDA-MB solution respectively (PDA final concentration: 100 μg mL^{-1}, equal to MB concentration: 10 μg mL^{-1}). At different intervals, 10 μL of the above solution was diluted to 150 μL with H_2O to test the concentration of GSH.

Photothermal Property of PDA-MB in Aqueous Solution. The photothermal conversion capability of PDA and PDA-MB were investigated by monitoring elevation of the temperature under the irradiation with 808 nm laser at 1.0 W cm^{-2}. 1 mL of PDA-MB solutions with different concentrations (0, 25, 50, 75, 100, 150, 200 μg mL^{-1}) were suspended in a cuvette and were exposed to 808 nm laser at 1.0 W cm^{-2} for 500 s. To investigate the photostability, the solution of PDA-MB (200 μg mL^{-1}) were irradiated by 808 nm laser for 500s, following by cooling down to room temperature. This procedure was repeated five cycles. The temperature of the solutions was recorded *via* digital thermometer per second. Meantime, the thermal images of PDA-MB solution were captured by infrared imaging camera (FOTRIC 225). Besides, the solution of PDA-MB (100 μg mL^{-1}) was irradiated by the laser with different laser powers (0, 0.5, 1.0, 1.5, 2.0, and 3.0 W cm^{-2}) for 500 s to investigate the effect of laser power.

Detection of ROS Levels in Aqueous Solution. 2',7'-Dichlorofluorescin diacetate (DCFH-DA), a frequently-used chemical ROS probe, was used to detect the ROS generation. Firstly, 10 μL of DCFH-DA (10 mM) in DMSO was added into 20 μL of NaOH (20 mM) to hydrolyze and produce 2',7'-dichlorofluorescin (DCFH) for 30 min. Then the above solutions were diluted to 200 μL of PB (20 mM, pH=7.2) to terminate hydrolysis. PDA-MB (100 μg mL^{-1}) and free MB (2 μg mL^{-1}) pretreated with or without GSH was added 5 μL of DCFH solution respectively. The mixture solutions were irradiated with 660 nm laser at 250 W cm^{-2} for 5 min. The fluorescence intensity of 2', 7'-dichlorofluorescein (DCF) at 512 nm was recorded after 5 min. Meantime, the fluorescence spectra of MB were acquired to calculate the concentration of MB in solution.

Cell Culture. Human cervical adenocarcinoma epithelial cells (HeLa) were cultured in DMEM supplemented 10% fetal serum and 1% penicillin-streptomycin. All cells were cultured at 37 ℃ in 5% CO_2 humidified environment. The culture medium was changed every two days, and the cells were digested by 0.25% trypsin-EDTA and re-suspended in fresh medium before plating.

Cell Viability Assay. Tetrazole (MTT) cytotoxicity assay was applied to evaluate cytotoxicity. HeLa cells were plated in 96-well plates with a density of 5×10^3 cells per well and allowed to adhere overnight. To investigate the cytotoxicity of as-prepared nanoparticles, different concentration (0, 10, 25, 50, 75, 100, 150, and 200 μg mL^{-1}) of PDA, PDA-MB and MB were added into each well of 96-well plates, and the cells were continued to be cultured for 24 h.

The cells were washed twice with PBS, and then 100 μL of 0.5 mg mL^{-1} of MTT stock solution in PBS was added into every plate and incubated for another 4 h. After removing the MTT, the 150 μL dimethyl sulphoxide (DMSO) was added to dissolve the intracellular formazan incubating for 30 min. The absorbance at 490 nm was recorded using the microplate reader. The cell viability was calculated by the ratio of the absorbance of blank group. The results were expressed as the relative viability of the non-treated cell. To investigate of the photothermal and photodynamic therapeutic efficiency *in vitro*, HeLa cells were incubated with PDA-MB (0, 25, 50, 75, 100, and 200 μg mL^{-1}) for 4 h. Later on, culture medium was removed and washed with PBS for three time. Then, the cells were exposed to the laser irradiation for 5 min (808 nm laser, 1 W cm^{-2}, 660 nm laser, 250 mW cm^{-2}) after removing the PDA-MB. The cell viability was measured by MTT after another 24 h. The results were expressed as the relative viability of cells only treated with irradiation.

Measurement of Intracellular GSH/GSSG Level. HeLa cells (1×10^5) were seeded in 6 well plates and adhered for 12 h. To regulate the level of GSH in cells, the cells were treated with NEM (10 μM) for 10 min, LPA (500 μM) for 24 h and PDA-MB for 4 h, respectively. After treatment, the cells were harvested, washed with PBS for three times. Then the intracellular GSH/GSSG ratio was measured using the GSH and GSSG Assay Kit (Beyotime, Jiangsu, China) according to the manufacturer's instructions.

Intracellular Fluorescence Imaging. For cellular uptake, HeLa cells (1×10^4) were plated at 20 mm confocal dish. After adherent overnight, PDA-MB (100 μg mL^{-1}) were added and

incubated for 0.5, 1, 2, 4 and 6 h respectively. Later on, culture medium was removed and washed with PBS three times. Then the cells were fixed with 1 mL 4% formalin for 15 min at 4 ℃ and later washed with PBS three times. Flowing that, 300 μL DAPI solution were added and incubated for 20 min. After washing three times using PBS, the confocal images were acquired by confocal laser scanning microscopy. The fluorescence of DAPI were measured with excitation at 405 nm and emission at 460 nm. The fluorescence of MB was measured with excitation at 640 nm and emission at 697 nm.

To evaluate the phototherapy efficiency of PDA-MB, HeLa cells (5×10^5) were seed in a culture dish and were adherent for overnight. Then the PDA-MB (200 μg mL^{-1}) were added and incubated for 4 h. Later on that, the cells were washed by PBS for three times and then irradiated with 808 nm laser at 1 W cm^{-2} and 660 nm laser at 250 mW cm^{-2} for 5 min. Afterward, the cells were co-stained with calcein acetoxymethyl ester (calcein-AM) (2 μM) and propidium iodide (PI, 3 μM) for 20 min. Then the cells were washed by PBS for three times and were subjected to confocal laser scanning microscope.

To investigate the intracellular ROS generation, HeLa cells were seeded into 12 microplates in 5% CO_2 at 37 ℃ to adhere overnight. Then the cells were treated with PBS and PDA-MB (100 μg mL^{-1}) under irradiation respectively, the treatment of NEM, PDA, PDA-MB without irradiation as contrast. After each well was then washed with PBS for three times, 200 μL of DCFH-DA (10 μM) was added into each well for 30 min at 37℃. The ester of DCFH-DA would be removed by esterase and the DCFH remaining part would be oxidized by ROS to produce

DCF, which had green fluorescence. After that, HeLa cells were washed by PBS to removing excessive DCFH-DA. Then the cells were subjected to Cytation 5 fluorescence microscope and the cell untreated with laser served as control.

To study the influence of intracellular GSH on the ROS generation, the LPA were induced into cells to up-regulate the GSH concentration before the incubation of PDA-MB and MB respectively and irradiation (250 mW cm^{-2}). In addition, the generation of ROS was measured the same as before.

Flow Cytometric Analysis. The cellular uptake was measured by flow cytometry. HeLa cells (5×10^5) were seeded in 6-well plates. After adherent overnight, the PDA-MB (100 μg mL^{-1}) were added and incubated different times (0.5, 1, 2, 4 and 6 h) respectively. Later on, the cells were washed with PBS for three times and digested by 0.25% trypsin-EDTA. Finally, the cells were suspended in 500 μL PBS and filtered through 300-mesh filter to remove the cell aggregates for flow cytometric analysis on the CytoFLEX S flow cytometer.

Cell apoptosis was studied using PI/Annexin V-FITC kit (BestBio) through flow cytometry. HeLa cells were seed at density of 2×10^5 cells per well in 6-well plates and grown overnight. After, cells incubated with PDA-MB for 4 h, and washed with PBS for three times. Cells were irradiated with the 660 nm laser at 250 mW cm^{-2} for 5 min and further exposed to an 808 nm laser at 1 W cm^{-2} for 5 min, cells without treatment served as controls. Then the cells were incubated for another 24 h. The cells were washed by PBS and digested by 0.25% trypsin. After centrifugation at 2000 rpm for 3 min, the cells were dispersed with 500 μL of binding buffer and

filtered through 300-mesh filter. The cells were kept in 4 ℃ and were stained with 5 μL Annexin-VI FITC for 15 min, and then 10 μL of PI for 5 min. The cells were prepared to flow cytometry analysis immediately. To investigate the influence of GSH on cell apoptosis, the cells were incubated LPA to improve intracellular GSH level. After 24 h, the cells were incubated with MB (2 μg mL^{-1}) and PDA-MB (100 μg mL^{-1}) for 4 h, respectively. The procedure of flow cytometry sample was treated as same as that of that of former one. After irradiation with 660 nm laser for 5 min, the cells were incubated for another 24 h. Cells were viewed in green channel for annexin V-FITC (λex = 488 nm, λem = 500~560 nm) and red channel for PI (λex = 561 nm, λem = 600~680 nm), respectively.

For intracellular ROS generation, the cells were incubated with DCFH-DA (10 μM) for 20 min at 37 ℃ after treating with PBS and PDA-MB (100 μg mL^{-1}) for 4 h respectively. Then the cells were irradiated under 660 nm laser at 250 mW cm^{-2} for 5 min and digested to disperse in PBS. The cell only treated with PBS, PDA, NEM and PDA-MB respectively without laser serve as control. The samples were subjected to flow cytometry analysis with excitation at 488 nm and emission at 500~540 nm.

To investigate the influence of GSH for intracellular ROS generation, the cells were incubated LPA to improve intracellular GSH level. After 24 h, the cells were incubated with MB (2 μg mL^{-1}) and PDA-MB (100 μg mL^{-1}) for 4 h, respectively. Then the cells were incubated with DCFH-DA (10 μM) for 20 min at 37 ℃ and irradiated under 660 nm laser at 250 mW cm^{-2} for 5 min. Finally, the cells were digested to disperse in PBS for fluorescence imaging.

Wound-Healing Assay and Transwell Invasion Assay. 4T1 cells (1×10^6 cells per well) were seeded into 6-well plates and cultured overnight in 5% CO_2 at 37℃. Then the cells were incubated with PDA-MB (100 μg/mL) for 4 h. After that, the cells were scratched with 200 μL pipette tip and washed with PBS to remove excessive PDA-MB and cells. The gap distance was observed at 0 h and 24 h under microscope after and before irradiation. Wound-healing assay were conducted as described. 2×10^5 4T1 cells were seed into the 6-well plate for 12 h. The cells were digested by 0.25% typsin after different treatment and dispersed in DMEM (2% FBS, 1% penicillin-streptomycin). The upper chamber was precoated with 1:40 dilution of matrigel for 24 h. Then, 100 μL of cells suspension were added to the upper chamber pretreated with the bottom chamber contained complete medium with 10% FBS. The cells in the upper chamber were allowed to invade Matrigel membranes for 24 h at 37 ℃ toward the bottom chamber. Cells were fixed in 4% paraformaldehyde and stained with 0.5% Crystal Violet Staining Solution. Cells in the upper chamber were removed with humidified cotton swab to quantify the number of invaded cells. Migrating cells on the other side of the membrane were photographed under a color bright field microscope (10×). The area covered by cells was quantified with Image J on at least four random fields per well.

***In Vivo* Inhibition of Primary Tumor.** The *in vivo* study was performed with protocols. BALB/c nude mice (5 weeks old, weight 18-22 g) were selected for establishing the xenograft human uterine cervical cancer cell (HeLa cells) tumor models. HeLa cells (1×10^7) in 50 μL of mixtures of matrigel and saline (1:1) were subcutaneously injected into the hind limb, and the

tumors were grown to uniform size of around 100 mm^3 after 4 weeks. Then the mice were randomly divided into five groups (five mice per group): (1) PBS, (2) PDA-MB, (3) PDA-MB plus 660 nm laser (250 mW cm^{-2}), (4) PDA-MB plus 808 nm laser (1 W cm^{-2}), (5) PDA-MB plus 660 nm and 808 nm laser. Each group was intravenously injected with 50 μL various solution (800 μg mL^{-1}, equal to 160 μg mL^{-1} MB) every 7 days. At 6 h post-injection, tumor on mice of treatment group was irradiated with 660 nm laser for 5 min and with 808 nm laser for 5 min. The tumor size was measured with digital calipers in two dimensions every two days. Tumor volumes were calculated by the formula: volume = (tumor length)*(tumor width)^2/2. The relative tumor volume was normalized to the initial volume (V/V_0, V_0 was initial volume). After the 15th day, all the mice were sacrificed, and the tumor was dissected. The tumor site was weight to evaluate the therapeutic effect.

Measurement of Intratumoral GSH/GSSG Ratio and ROS Level. Tumor-bearing mice were received different treatment. After intravenous injection at 24 h, all the mice were sacrificed, and the tumor was dissected. The tumor tissues were homogenized with a homogenizer for measuring GSH/GSSG ratio according to the manufacturer's instructions of GSH and GSSG assay kit (Beyotime, Jiangsu, China). ROS level was measured by DCFH-DA staining. The tumor tissue was frozen at -80 ℃ and stained by DCFH-DA and DAPI on frozen section, and then subjected to fluorescence imaging.

***In Vivo* Inhibition of Metastatic Cancer.** All animal experiments were carried out according to the Principles of Laboratory Animal Care (People's Republic of China). The animal

protocol was approved by The Institutional Animal Use and Care Committee of Wuhan University. To develop the orthotopic metastatic breast cancer model, 2×10^5 4T1 cells were planted into the third mammary pad of each nude mice. When the tumor volumes reached around 100 mm^3, the mice dived into five group: (i) PBS, (ii) PDA-MB, (iii) PDA-MB plus 660 nm laser, (iv) PDA-MB plus 808 nm laser and (v) PDA-MB plus 660 nm and 808 nm laser. For each group was intravenously injected with 50 μL various solution (800 μg mL^{-1}, equal to 160 μg mL^{-1} MB) every 7 days. At 6 h post-injection, tumor on mice of treatment group was irradiated with a 660 nm laser for 5 min and with 808 nm laser for 5 min. The lung tissues were removed and photographed after 28 days. And the number of macroscopic metastatic nodules per lung was recorded. H&E staining was used for histological examination of lung tissues in each group to detect lung metastasis.

***In Vivo* Fluorescence, Photoacoustic, and Thermal Imaging.** To investigate fluorescence image, tumor-bearing mice used for imaging were intravenously injected with PDA-MB solution (50 μL, 800 μg mL^{-1}). After that, fluorescence of the mice was observed at several specific time points by using IVIS imaging system. After 24 h, the tumor and major organs were collected from the sacrificed mice for imaging by an IVIS imaging system.

To study *in vivo* the PA imaging property of PDA-MB, the tumor-bearing mice were intravenously injected with 50 μL of PDA-MB solution (800 μg mL^{-1}). Then the mice were scanned with PA imaging system at tumor sites to obtain PA signals at several specific time points. The wavelength of the laser was fixed at 744 nm and 523 nm.

To investigate the *in vivo* thermal imaging potential, tumor-bearing mice were divided into two groups and intravenously injected with PDA-MB solution (50 μL, 800 μg mL^{-1}) and PBS, respectively, and exposed to 808 nm laser at 1 W cm^{-2} for 5 min followed by imaging using an infrared (IR) thermal camera.

Histopathological Examination. At the 15th day, mice with different treatment were sacrificed, and the main organ (heart, liver, spleen, lung, and kidney) were dissected. The main organs and tumor were fixed in 10% neutral buffered formalin to process routinely into paraffin. Then both the organ tissues and tumors were sliced to 4 μm thickness for hematoxylin and eosin (H&E) staining, and the slices were observed by fluorescence microscope.

Immunohistochemistry and terminal deoxynucleotidyl transferase-mediated dUTP-biotin nick end labeling assay (TUNEL). VEGF expression levels in the tumor tissue were confirmed by immunohistochemistry. After predetermined times, mice were sacrificed and tumor tissues were harvested and fixed in 10% neutral buffered formalin and processed routinely into paraffin. Slices were stained with antibody overnight at 4 ℃. A streptavidin-biotin–peroxidase complex with diaminobenzidine was used to visualize immunoreactivity by the manufacturer's instructions. The results were evaluated according to the average optical density value. Apoptotic cell death in the tumor tissue was measured using terminal deoxynucleotidyl transferase-mediated dUTP-biotin nick end labeling assay (TUNEL) using an *in situ* cell death detection kit (Roche) according to the manufacturer's protocol. Images were acquired using fluorescence microscope.

Serum Biochemistry Test. Blood sample were collected *via* the orbit after receiving different treatment for 14 days (1 mL, $n = 3$). To acquire the serum sample, the blood was centrifuged with 5000 rpm for 5 min. Serum levels of alkaline phosphatase (AKP), glutamic-pyruvic transaminase (GPT), glutamic oxaloacetic transaminase (GOT), creatine kinase (CK), creatinine (CRE) and uric acid (UA) were measured using the commercial serum biochemistry test kits.

Statistical Analysis. Statistical significance was calculated by Student's *t*-test: $^{***}P < 0.001$, $^{**}P < 0.01$, $^{*}P < 0.05$, ns, not significant.

Supplementary figures and tables

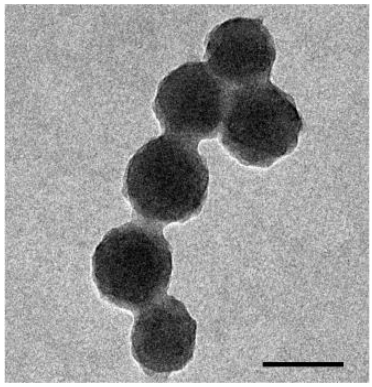

Fig. S1 TEM image of PDA. Scale bar: 100 nm.

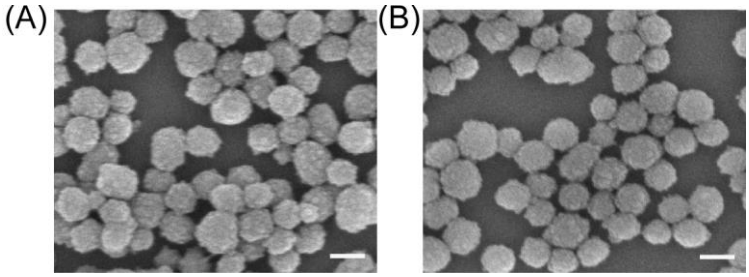

Fig. S2 SEM images of PDA (A) and PDA-MB (B). Scale bar: 100 nm.

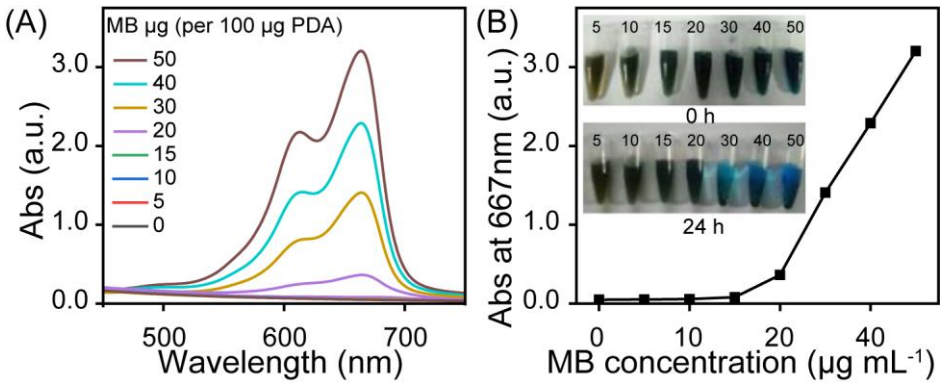

Fig. S3 (A) UV-vis absorption spectra of PDA-MB supernatant after incubating a fixed level of PDA with different feed ratio of MB. (B) Plot of the absorbance intensity at 667 nm versus MB concentration. Inset: Photograph of PDA-MB suspension (MB concentration: 5, 10, 15, 20, 30, 40, 50 μg mL^{-1}; PDA: 100 μg mL^{-1}).

Fig S3A was the UV-vis absorption spectra of the PDA-MB supernatant (the residual MB) obtained by using different MB/PDA ratios to synthesize PDA-MB. Fig S3B was the plot of UV-vis absorption intensity at 667 nm versus the added MB concentration as indicated in Fig S3A. By adjusting the MB feed ratio, the loading efficiency of PDA reached up to 91.35% when utilizing 20 μg mL^{-1} MB and 100 μg mL^{-1} PDA (MB_{weight}: PDA_{weight}=1:5) for PDA-MB synthesis, while bigger MB/PDA ratio could result in aggregation (inset images of Fig S3B).

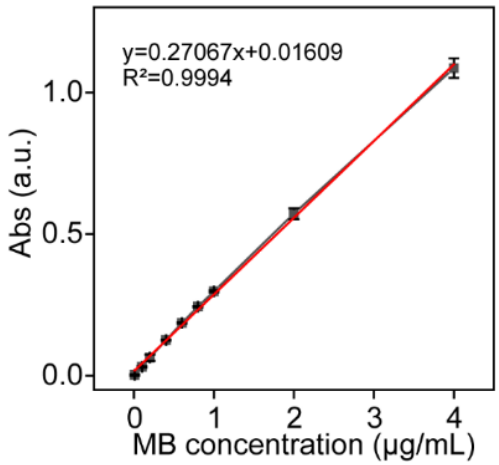

Fig. S4 Linear relation between absorption at 667 nm and MB concentration.

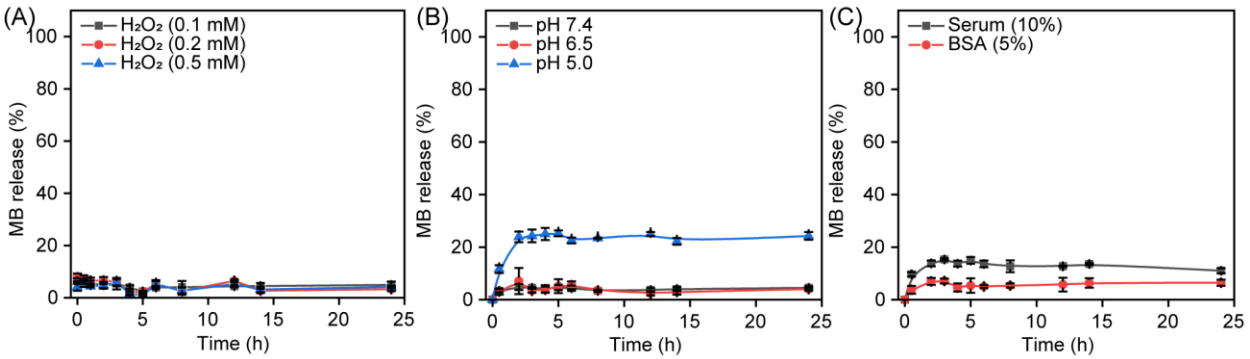

Fig. S5 (A) Time-dependent release of MB from PDA-MB in the presence of different concentrations of H_2O_2. (B) Time-dependent release of MB from PDA-MB at different pH. (C) Time-dependent release of MB from PDA-MB in serum and BSA medium. PDA-MB: 100 μg mL^{-1}.

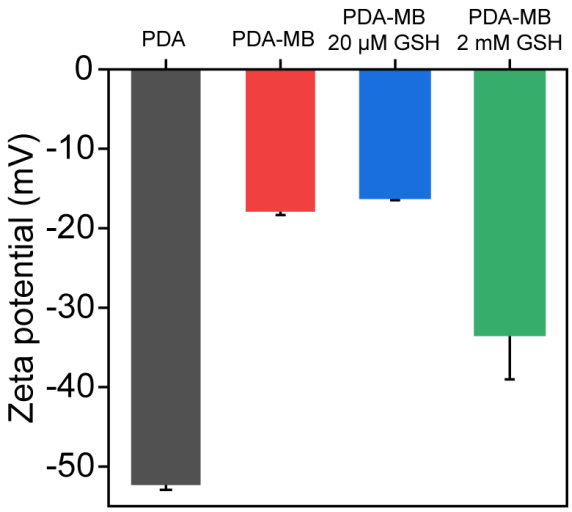

Fig. S6 Zeta-potential of PDA, PDA-MB, and the mixture of PDA-MB and GSH. PDA-MB is incubated separately with 20 μM and 2 mM GSH for 30 min. PDA, 100 μg mL^{-1}. PDA-MB, 100 μg mL^{-1}.

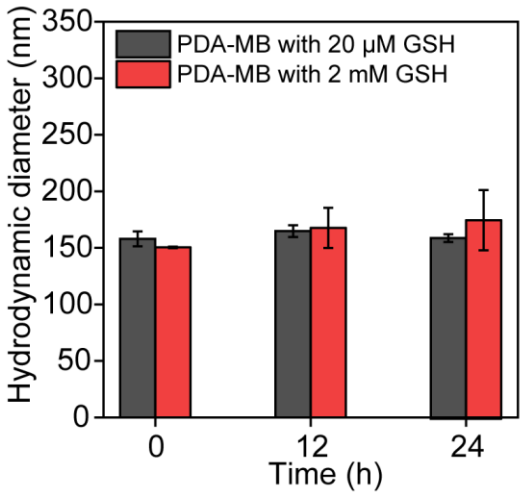

Fig. S7 DLS analysis of the hydrodynamic diameter of PDA-MB incubated with GSH (0.02 or 2 mM) for different times.

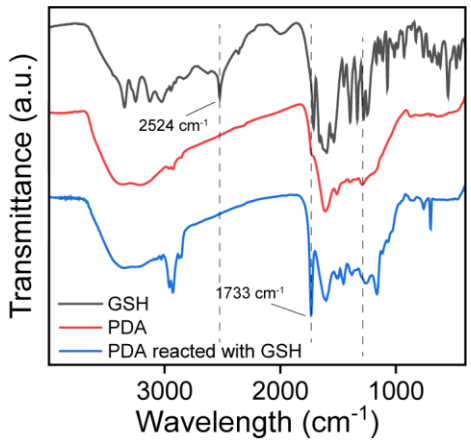

Fig. S8 FTIR spectrum of GSH, PDA, and the PDA adduct via the combination between PDA and GSH.

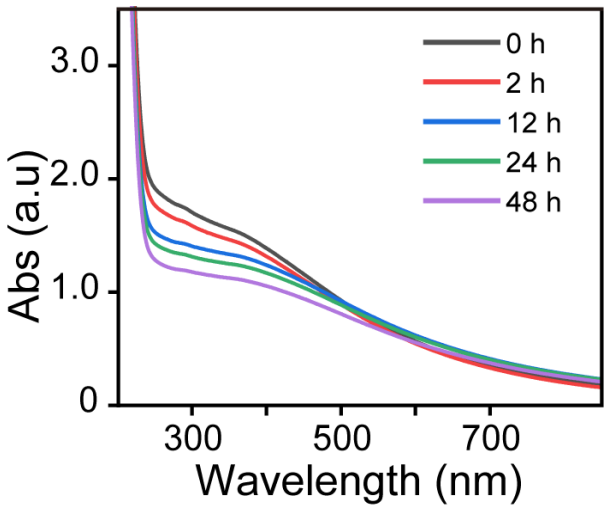

Fig. S9 The UV-vis absorption spectra of PDA after reaction with GSH for 0, 2, 12, 24, and 48 h respectively. PDA concentration: 100 μg mL^{-1}.

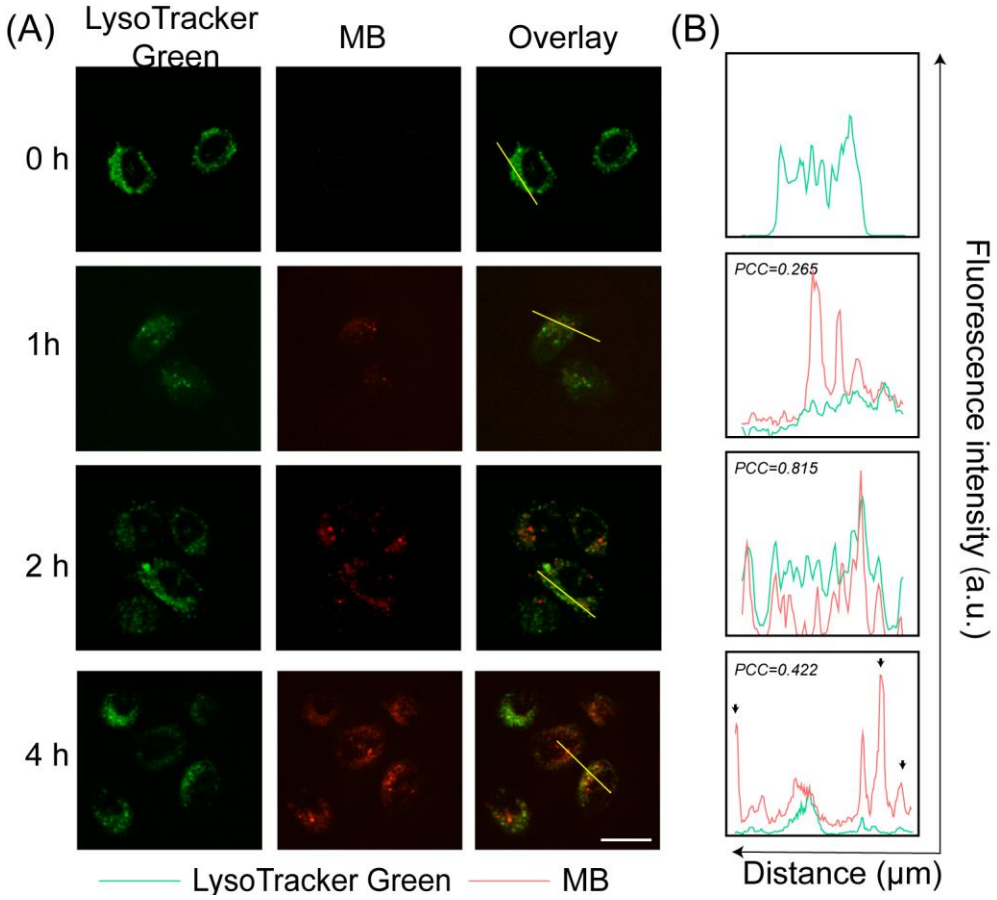

Fig. S10 Intracellular colocalization analysis of MB and Lysotracker Green in live HeLa cells. (A) Fluorescence images of HeLa cells. (B) Intensity profiles of the region of interest (yellow line indicated in (A)) exemplify degree of colocalization of LysoTracker Green (green) and PDA-MB (red). Scale bars, 26 μm.

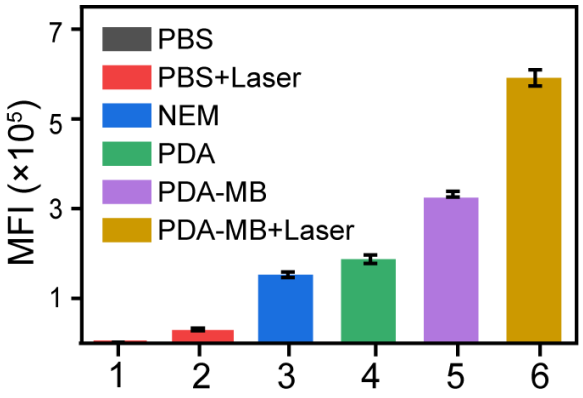

Fig. S11 Flow cytometry analysis of ROS levels in HeLa cells with various treatments as illustrated in Fig 5A. MFI represents mean fluorescence intensity.

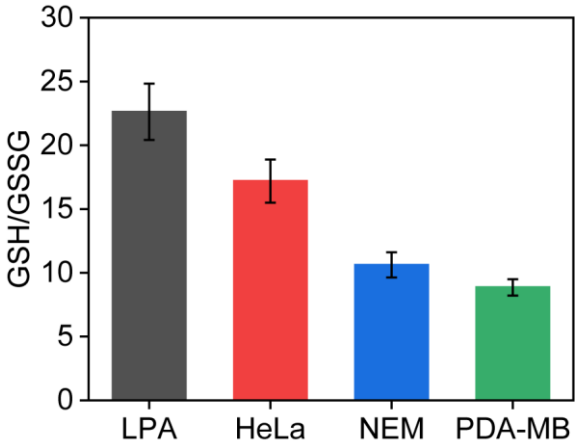

Fig .S12 GSH/GSSG ratio in HeLa cells incubated with LPA (500 μM), PBS, NEM (10 μM) and PDA-MB (100 μg mL^{-1}), respectively.

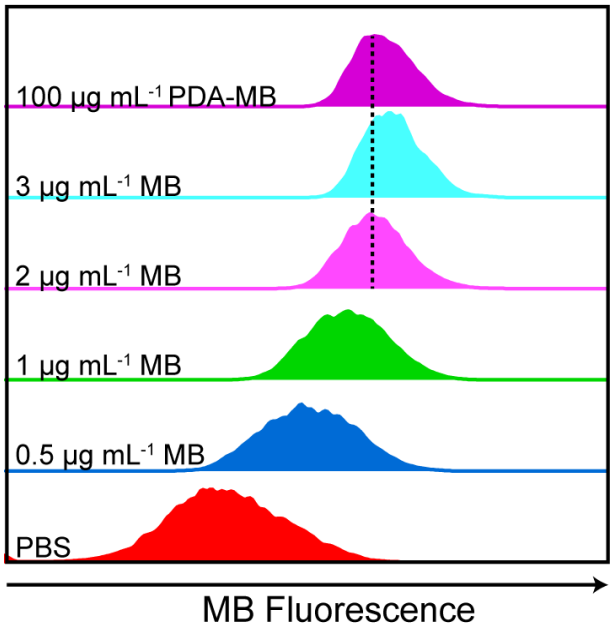

Fig. S13 Flow cytometry analysis HeLa cell treated with PDA-MB and different concentration of MB. PDA-MB concentration: 100 μg mL^{-1}.

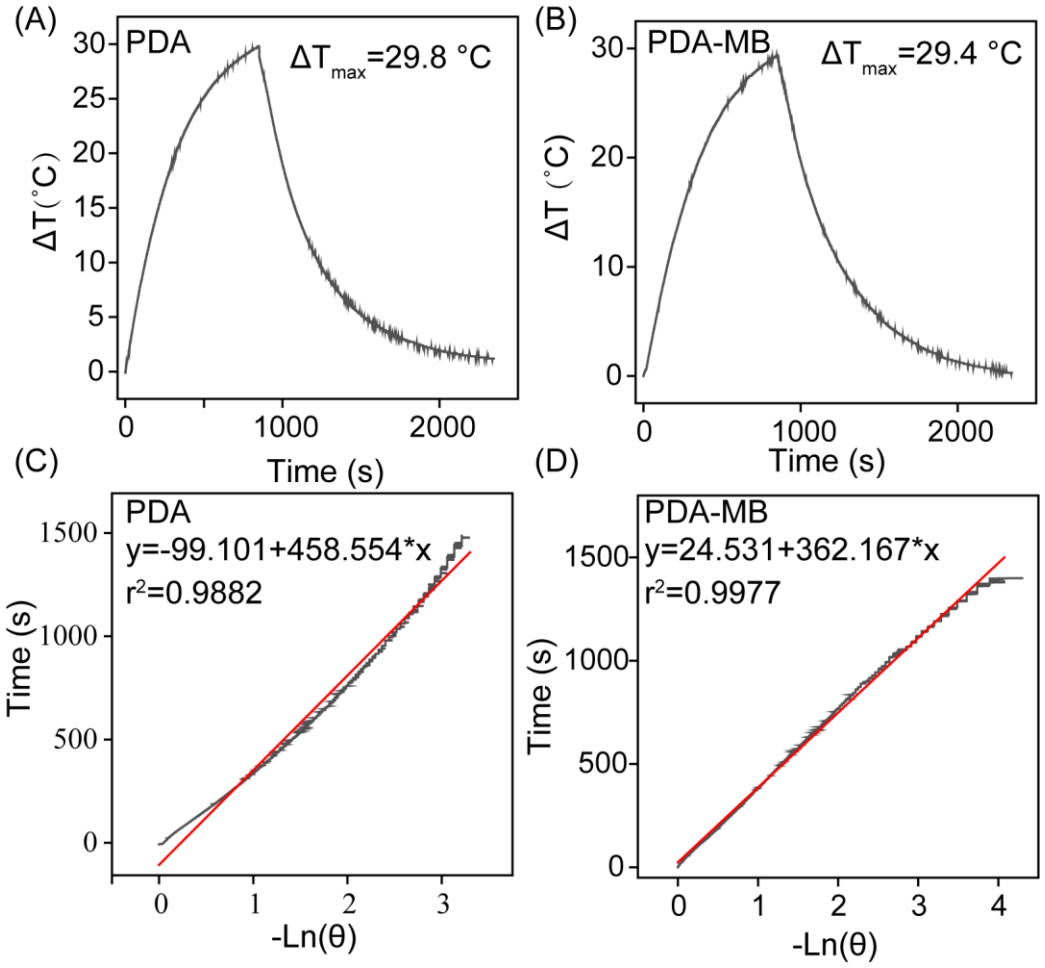

Fig. S14 (A,B) Temperature changes of aqueous PDA and PDA-MB (200 μg mL^{-1}) upon the photothermal ablation with 808 nm laser (2 W cm^{-2}) for 500 s and the subsequent removing of the laser. (C,D) Linear time data versus -lnθ obtained from the cooling period of (A) and (B).

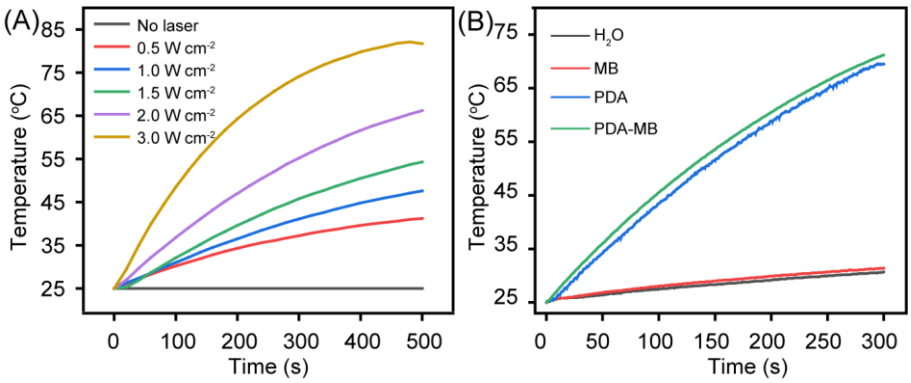

Fig. S15 (A) Photothermal curves of under laser irradiation with different laser power. (B) Photothermal property of H_2O, MB, PDA, and PDA-MB. PDA concentration:100 μg mL^{-1}. PDA-MB: 100 μg mL^{-1}. MB: 20 μg mL^{-1}.

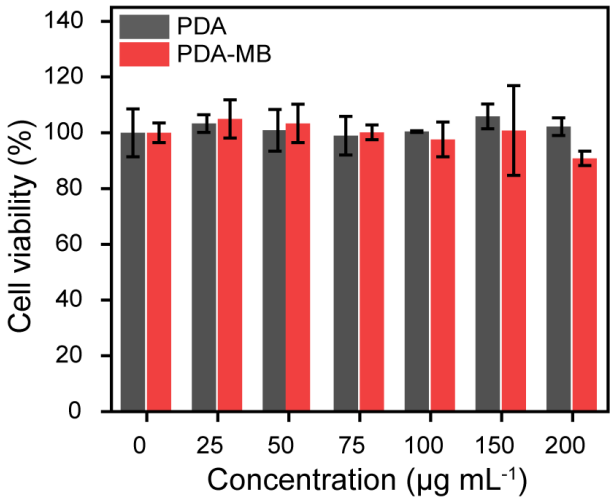

Fig. S16 Relative cell viability after different treatments, including PDA, PDA-MB and MB. (PDA: 0, 25, 50, 75, 100, 150 and 200 μg mL^{-1}, equal to MB concentration: 0, 5, 10, 15, 20, 30 and 40 μg mL^{-1}).

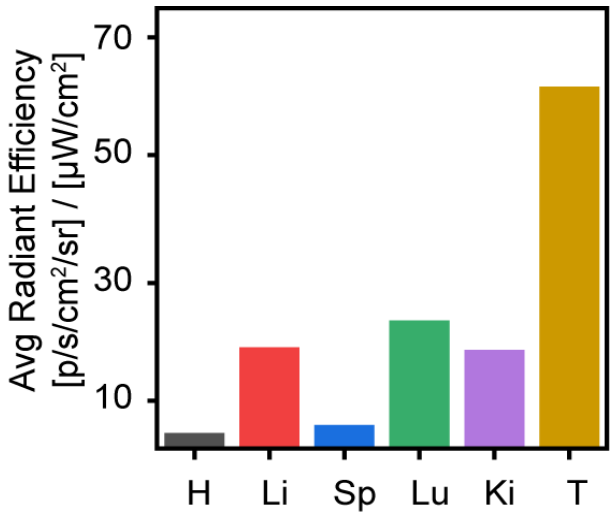

Fig. S17 Mean fluorescence intensity of PDA-MB in organs and tumour 24 h after intravenous injection. H, Li, Sp, Lu, Ki and Tu represented as heart, liver, spleen, lung, kidney and tumour respectively.

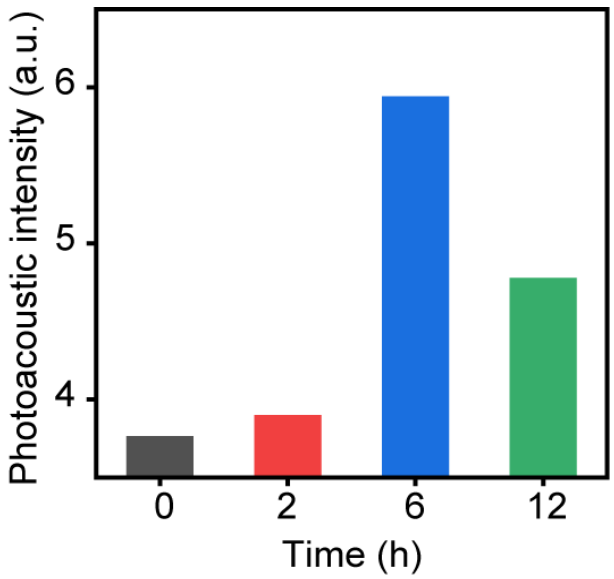

Fig. S18 Quantitative analysis of photoacoustic intensity at tumour site in Fig 8B.

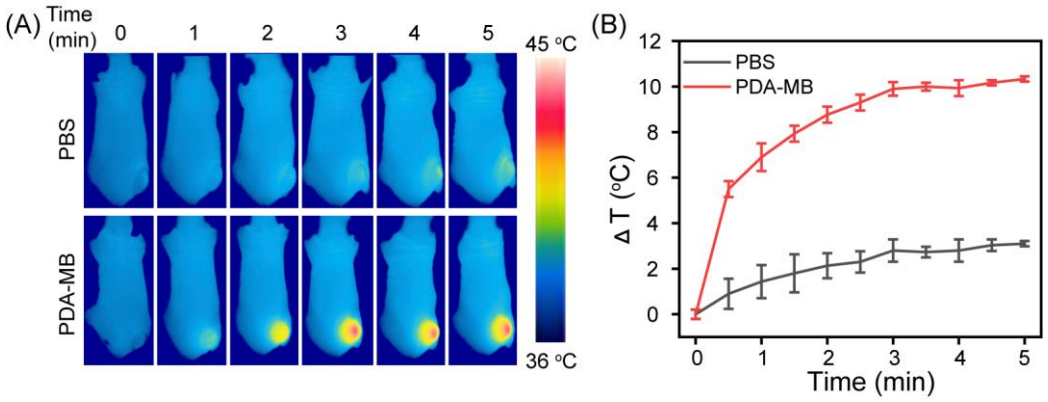

Fig. S19 (A) Thermographic images of tumor regions against time under NIR laser irradiation. (B) Temperature curves of tumor regions against time under laser irradiation. Laser, 808 nm; laser power, 1.0 W cm^{-2}.

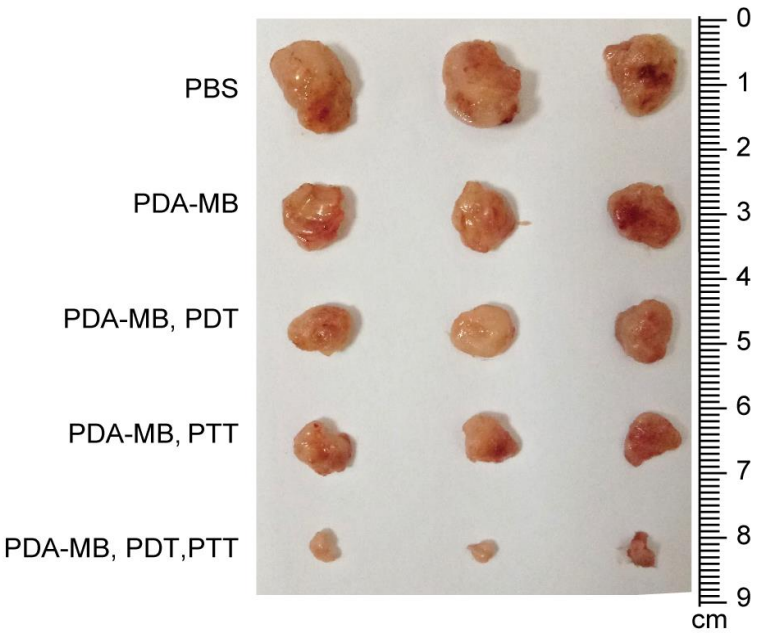

Fig. S20 Representative tumor images of different groups after 15 days' treatment.

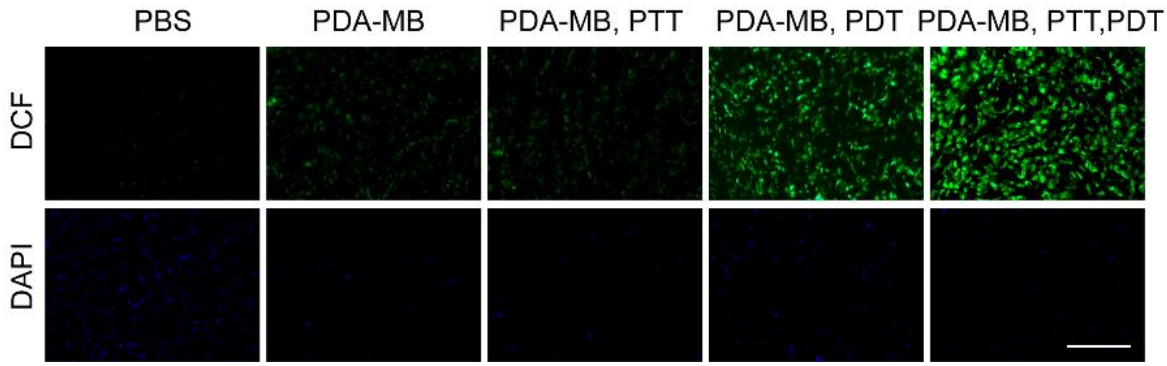

Fig. S21 DCF staining of tumor sections harvested from mice with different treatment at 24 h post-injection with PDA-MB. Scale bar: 100 μm.

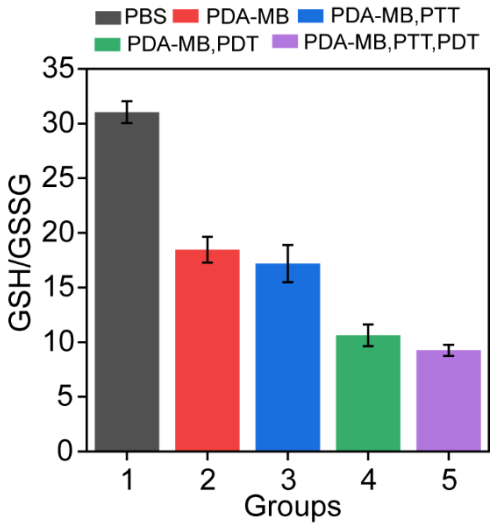

Fig. S22 GSH/GSSG ratio in tumor tissue homogenate collocted from mice with different treatment at 24 h post injection with PDA-MB.

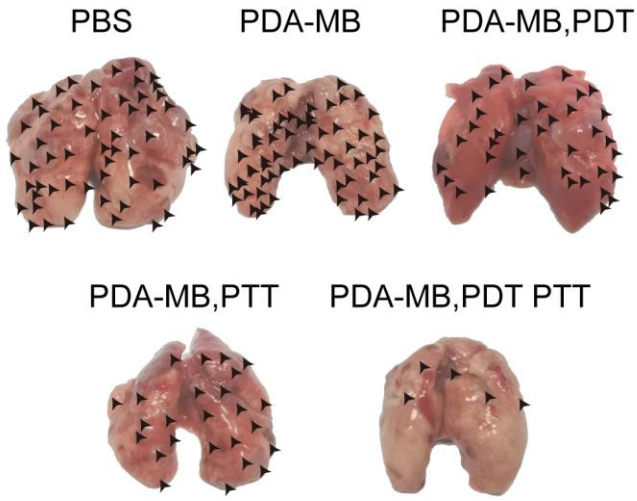

Fig. S23 Representative lung photographs of the mice received different treatment. Black arrows indicated the metastatic nodules.

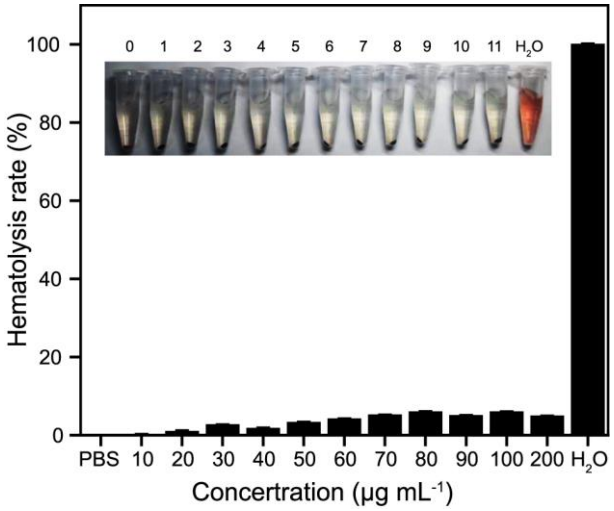

Fig. S24 Hemolytic activities of PDA-MB. Percentage of hemolysis was measured by a spectrophotometer. Inset photographs were corresponding to the RBCs exposed to different concentrations of PDA-MB in PBS. Numbers 0-11 represent different concentration of PDA-MB (from left to right: 0, 10, 20, 30, 40, 50, 60, 70, 80, 90, 100, and 200 μg mL^{-1}). H_2O was used as positive control.

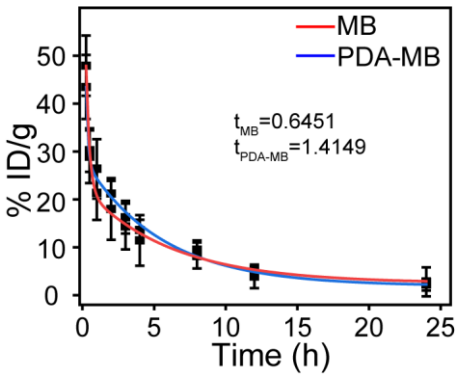

Fig. S25 The blood clearance kinetics of MB and PDA-MB after intravenously administration.

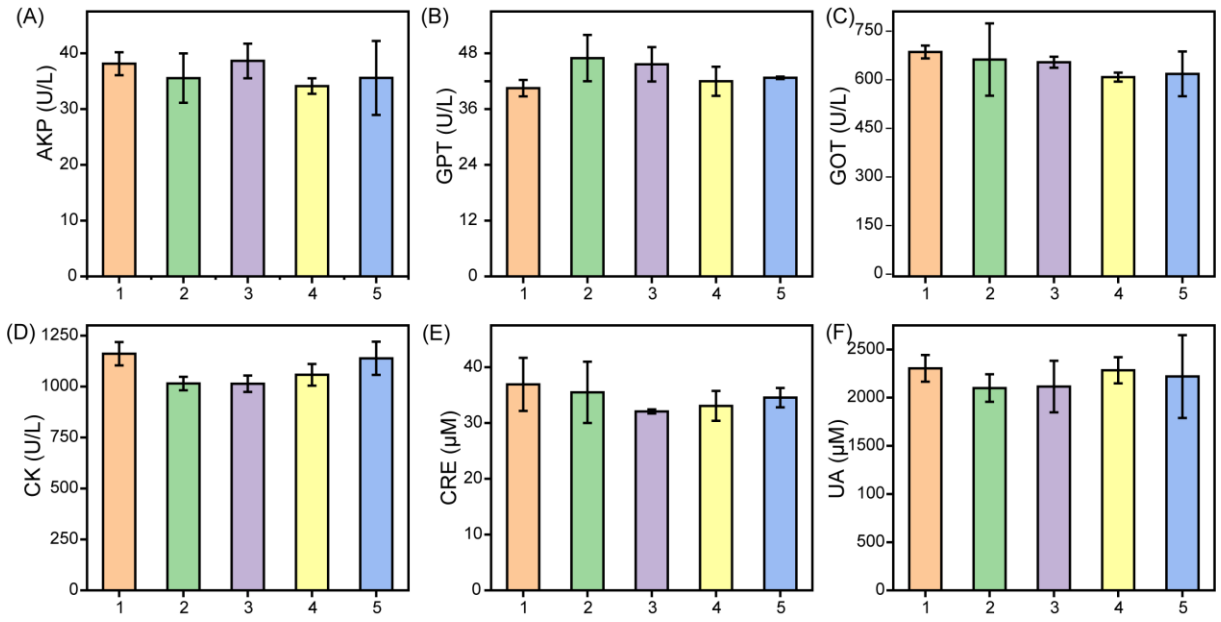

Fig. S26 Six typical blood biochemical indexes of tumor-bearing mice receiving different treatments for 14 days. (A) alkaline phosphatase (ALP); (B) glutamate-puruvate transaminase (GPT); (C) glutamic oxalacetic transaminase (GOT); (D) creatine kinase (CK); (E) creatinine (CRE); (F) urine acid (UA). Group 1-5 was PBS, PDA-MB, PDA-MB plus PDT, PDA-MB plus PTT and PDA-MB plus PDT and PTT.

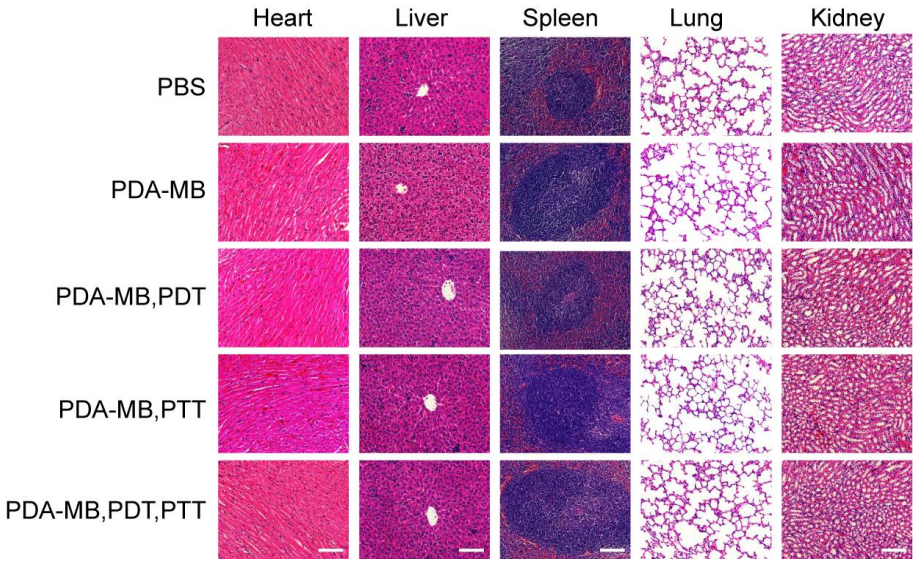

Fig. S27 H&E staining of heart, liver, spleen, lung, and kidney tissue slices from tumor-bearing mice receiving different treatments for 15 days. (Scale bar = 100 μm).

Table S1. The parameter values and photothermal conversion efficiency (η) of PDA and PDA-MB.

	$\sum_i m_i C_{p,i}$	hA	ΔT_{max}	A_λ	$I(1-10^{-A_\lambda})$	η(%)
PDA	4.2	0.00916	29.8	0.3864	0.589	41.51%
PDA-MB	4.2	0.01159	29.4	0.5808	0.738	42.76%

References

1. Y. Chen, K. Ai, J. Liu, X. Ren, C. Jiang, L. Lu, Biomaterials, 2016, 77, 198-206.